Journal of Applied Fluid Mechanics, Vol. 17, No. 2, pp. 398-409, 2024.
Available online at www.jafmonline.net, ISSN 1735-3572, EISSN 1735-3645.
https://doi.org/10.47176/jafm.17.02.2168

A Three-dimensional CFD Study on Multiphase Flow in an FCC Regenerator Integrated with Oxy-combustion

A. Erdoğan†

Advanced Materials Research Group, University of Nottingham, Nottingham, NG72RD, United Kingdom
Mechanical Engineering, Inönü University, Malatya, 44280, Türkiye

†*Corresponding Author Email: Ahmet.Erdogan@nottingham.ac.uk*

ABSTRACT

A vital process for converting heavy petroleum productions is Fluid Catalytic Cracking (FCC). As a major source of CO_2 emissions, the regenerator reactor in the FCC unit accounts for about 20-35% of the refinery's total emissions. A common method for reducing CO_2 emissions from the FCC regenerator is oxy-combustion, which has different advantages with regard to reducing energy penalties and associated costs. In this study, a computational fluid dynamic (CFD) study was used to examine the hydrodynamic characteristics of solid particles and gas inside the FCC regenerator, allowing CO_2 to be captured more efficiently. Utilizing Ansys Fluent platform, the Eulerian-Eulerian model was applied with granular flow kinetic theory. In the simulations, different mesh sizes were tested, and the hydrodynamics of the oxy-combustion regenerator were evaluated by adjusting CO_2 flow rates to achieve similar fluidization behaviors. The CFD results indicated that the conventional drag model accurately predicted the density phases within the bed. In oxy-combustion, CO_2, due to its density, naturally creates a smaller dense phase compared to air-combustion. Moreover, optimizing the fluidizing gas velocities resulted in enhanced particle mixing, resulting in a distributed flow with vortices within the dense phases due to a reduction in gas velocity. To improve the environmental performance of the FCC unit, this research provides valuable insight into the hydrodynamics of solid catalysts used in the oxy-combustion process.

Article History

Received July 15, 2023
Revised September 10, 2023
Accepted October 3, 2023
Available online December 4, 2023

Keywords:

Oxy-combustion
Computational Fluid Dynamic
Hydrodynamic
Multiphase flow
Regenerator

1. INTRODUCTION

Solid-gas multiphase flow is a complex phenomenon involving both gas and solid particles, encountered in many processes such as combustion (De Mello et al., 2013; Li & Shen, 2022), fluidized bed reactors (Cui & Grace, 2007; Hashim et al., 2020), pneumatic conveying (Aboudaoud et al., 2023; Chu & Yu, 2008; Rautiainen et al., 1999), spraying (Mezhericher et al., 2012; Zhang et al., 2021; Chen et al., 2022), and electro winning (Pourahmadi & Talebi, 2020). Among these processes involving solid-gas multiphase flows, fluidized bed reactors have excellent mixing and heat transfer characteristics, and they are therefore widely used in petrochemicals (Taghipour et al., 2005). One instance related to petrochemical applications of the fluidized bed reactors to consider is Fluid Catalytic Cracking (FCC), which assumes a crucial significance in converting vacuum gas oil or heavy petroleum residues to valued products such as light cycle oil, gasoline, and light petroleum gas (Tang et al., 2017a, b; Güleç & Okolie, 2023). However, a typical refinery produces approximately 20-30% of its overall gas emissions from fluid catalytic cracking (FCC), an important contributor to greenhouse gases (De Mello et al., 2013; Güleç et al, 2023a). There have been multiple proposals put forward to capture the CO_2 emissions from FCC units. These include Chemical Looping Combustion (CLC) (Güleç et al., 2019; Güleç et al., 2020a, b, 2023b), post-combustion capture (Digne et al., 2014; Miracca & Butler, 2015), and oxy-combustion capture (Da Silva et al., 2015; Dos Santos et al., 2008).

In this study, among these CO_2 capturing methods, oxy-combustion integrated with FCC is considered to investigate the solid-gas multiphase flow.

An FCC unit comprises of two interconnected reactor arrangements: a regenerator, known as a fluidized bed reactor, and a catalytic cracking riser, also referred to as a riser reactor (Jones & Pujadó, 2006). The preheated petroleum feedstock mixes with hot catalysts and steam

NOMENCLATURE

C_d	drag force	σ_k	turbulent Prandtl numbers
CFD	Computational Fluid Dynamic	σ_ε	turbulent Prandtl numbers
CLC	Chemical Looping Combustion	λ_s	bulk viscosity (solid)
CO_2	carbon dioxide	λ_s	bulk viscosity (gas)
FCC	Fluid Catalytic Cracking	Θ	granular temperature
O_2	oxygen	g_i	gravity acceleration
a	volume fraction	g_0	radial distribution function
ε	turbulence dissipation ratio	h	bed height
k	turbulence kinetic energy	P	pressure
μ	dynamic viscosity	$\vec{v}$	instantaneous velocity
$\mu_{t,g}$	turbulence viscosity (gas)	v'	fluctuating velocity (solid)
$\mu_{eff,g}$	effective viscosity of gas phase	Γ_Θ	granular diffusion coefficient
μ_s	shear viscosity (solid)	Π_g	turbulent exchange terms (gas)
ρ	density	Π_k	turbulent exchange terms (solid)

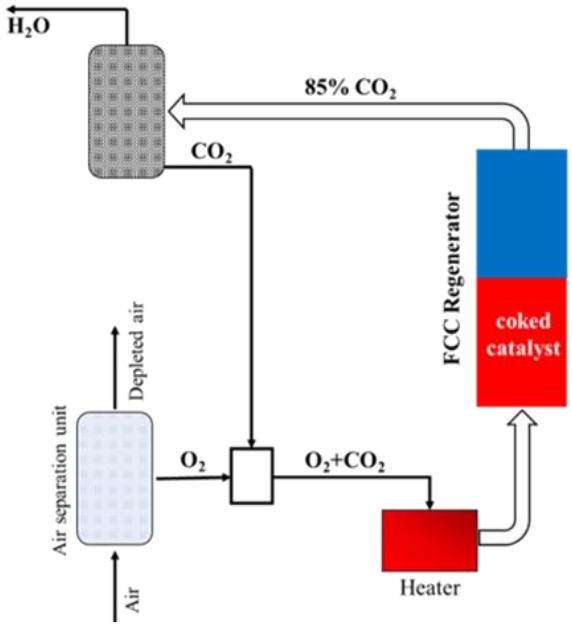

Fig. 1 Flow chart of oxy-combustion process in the FCC (Güleç et al., 2020a)

and is cracked at a temperature of 480-600 °C in the FCC riser reactor (Güleç, et al., 2023c). Once the catalyst surface accumulates coke, primarily in the form of carbon, the catalyst activity decreases. In cyclones, cracked products and coke-deposited catalysts are separated after cracking reactions. After moving the coke-containing catalyst to the regenerator, the coke within the FCC regenerator is eliminated by using oxygen (O_2) to burn.

A regenerator utilizing high purity oxygen is used for CO_2 capture in oxy-combustion processes to produce a fuel gas primarily containing CO_2 and H_2O vapor. Figure 1 illustrates the oxy-combustion process in the FCC. During the dehydration process, recycled CO_2 obtained from the air separation unit (ASU) is mixed with pure oxygen supplied. A combination of O_2 and CO_2 is then directed to the regenerator, where it is burned off to remove the coke that accumulated on the FCC catalyst. In order to complete the regeneration process, the coke is burned on the catalyst with oxygen. A crucial important step within the FCC unit is this regeneration process, which involves solid-gas multiphase flows (Azarnivand et al., 2018). The effectiveness of catalyst regeneration in the regenerator depends on the level of distribution and thorough mixing of the catalytic materials with the gas. In this stage, it becomes clear that the hydrodynamics involved in the flow of the solid-gas multiphase system within the FCC regenerator are of considerable importance.

A computational fluid dynamic (CFD) model provides a lot of information about the fluid domain, such as velocity, pressure, temperature, turbulence, and particle volume fraction (Kamer et al., 2018; Erdoğan & Daşkın, 2023; Karabulut, 2023a, b; Lu et al., 2023). Consequently, the utilization of CFD studies has progressively grown in importance for the design, analysis, and optimization of FCC regenerators. Particles volume fraction and bed density in the regenerator are commonly regarded as the indicators of the hydrodynamic characteristics in the FCC regenerator, pertaining to the flow of solid-gas multiphase systems. Fluidized bed reactors, which are samples of solid-gas multiphase flows, are commonly studied using CFD (Khan et al., 2014). Furthermore, CFD has been used extensively to predict hydrodynamics (Schwarz & Lee, 2007; Li et al., 2009; Alzate Hernández, 2016; Azarnivand et al., 2018; Güleç et al., 2021; Yang et al., 2021b), coke combustion (Zimmermann & Taghipour, 2005; Chang et al., 2013; Amblard et al., 2017; Berrouk et al., 2017; Singh & Gbordzoe, 2017; Yang et al., 2021a;), and heat transfer (Amblard et al., 2017) in FCC regenerators.

Güleç et al. (2021) studied the hydrodynamic of the CLC-FCC regenerator. They revealed effects of some parameters such as superficial gas velocity, gas inlet geometry, flow regimes, and drag models on the solid-gas mixing performance and bed density profiles. It should be noticed that the study focused on the Chemical Looping Combustion (CLC) process. Some computational studies have been conducted on the air-combustion process in different regenerator geometries to investigate their hydrodynamic performance. Gao et al. (2009) reported the hydrodynamic of the air-combustion process in the FCC regenerators. They revealed that flow models and kinetic theories are less sensitive to the coefficient of restitution than hydrodynamics. In the study carried out by Chang et al. (2016), it was computationally revealed that two regions, are dense region and a dilute region, occurred in the regenerator used for regeneration of the catalysts

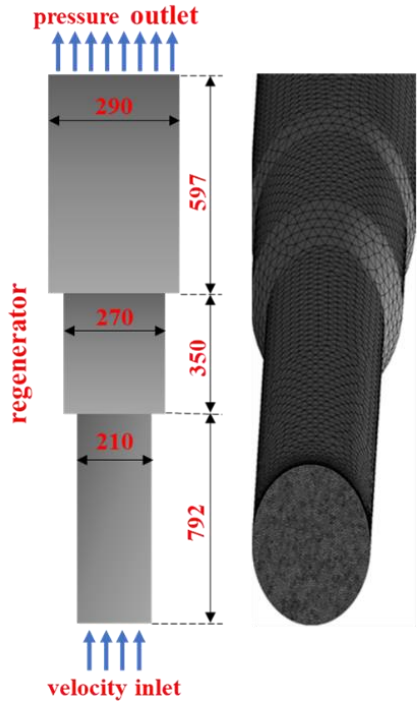

Fig. 2 The geometric (in mm) and boundary conditions details of regenerator solid model

coked. In another study (Chang et al., 2016), CFD modeling was used to analyze gas-solid flow patterns in a laboratory-scale fluid catalytic cracking regenerator, highlighting the impact of recirculated catalyst and airflow velocity on catalyst distribution. As a result, oxy-combustion processes have not been numerically studied in the FCC regenerator since the fluidization gas is mainly air or CO_2 in chemical looping combustion.

Specifically, this study aims to comprehensively investigate the hydrodynamic attributes of the FCC unit's regenerator, focusing on how CO_2 is captured during the oxy-combustion process. The Syamlal-O'Brien drag model, which has never been used for oxy-combustion, was used to simulate and analyze the performance of the FCC regenerator during the oxy-combustion process, focusing on elucidating the hydrodynamic characteristics of the solid-gas mixture. A series of bed density values, volume fraction contours, and velocity vectors of the solid particles (catalysts) were obtained for different flow times and were compared.

2. CFD METHODOLOGY

2.1 Geometry and Mesh Details

Firstly, a solid model was developed in three dimensions to simulate the solid-gas multiphase flow which occurs in the FCC regenerator under conditions of oxy-combustion to simulate the FCC regeneration process. Fig**ure** 2 depicts the geometric details and mesh model of the regenerator. The regenerator was simplified with a downscale of 1/10 in order to avoid simulation cost and time (Güleç et al., 2021). There are three sections to the regenerator unit, each with a different diameter and height. At the bottom, the diameter is 210 mm, and the mm, respectively. As the middle section of the CLC-FCC

Table 1 Mesh numbers

Mesh code	Number of mesh elements
M1	150000
M2	220000
M3	300000
M4	430000
M5	520000

regenerator model measures 350 mm in height, the upper height is 792 mm. The middle section and an upper section have diameters of 270 mm and 290 mm, respectively. Ansys-Fluent, a commercial software package, is used to conduct the CFD simulations. So as to discretize the spatial of the FCC regenerator fluid domain, the Finite Volume Method is used. Also, it can display velocity, pressure, temperature, shear stress, and volume fraction for fluid domains. An analysis of a three-dimensional multiphase flow based on CFD simulations of granular flows is presented in this research, utilizing the Eulerian-Eulerian model and incorporating the kinetic theory of granular flows. It was demonstrated in this study that all CFD simulations were performed with triangle meshes as the meshing geometry.

In order to ensure that the mesh structure is suitable for numerical simulations using CFD, mesh independence studies are required. A mesh independence study was conducted using five different mesh numbers and simulations to measure the effectiveness of mesh independence. The mesh numbers identified in the mesh independence study are listed in Table 1.

The solid-gas multiphase flow is significantly influenced by the entrance zone because most of the interaction between solid and gas phases occurs in this specific region of the FCC regenerator. Hence, dense meshes are created in the inlet area so that more sensitive solutions can be obtained. An acceptable value of 0.77 (Fluent, 2009) was reached for maximum skewness, an important metric for mesh quality evaluation. Meshes are refined across the entire flow domain. A mesh curvature of 18 degrees is implemented, with coarse and medium settings chosen for the relevance center and mesh smoothing characteristics.

2.2 Numerical Approach

The turbulent flow of a mixture of solid particles and gas is simulated by creating a multiphase fluid dynamics model that employs the Eulerian-Eulerian framework to represent solid and gas phases. Using averaged equations, it is possible to extend these models to simulate solid-gas multiphase flow for the oxy-combustion process in the FCC regenerator. Both the solid and gas phases are subject to the application of conservation principles for mass, momentum, and granular temperature independently. The regenerator's flow of solid particles and gas is described by utilizing a computational fluid dynamics (CFD) model. This model incorporates a multiphase flow approach based on the granular flow kinetic theory, allowing for the derivation of the governing equations. The granular temperature undergoes temporal and spatial variations within the bed, thereby influencing the viscosity and stress characteristics of the solid phase.

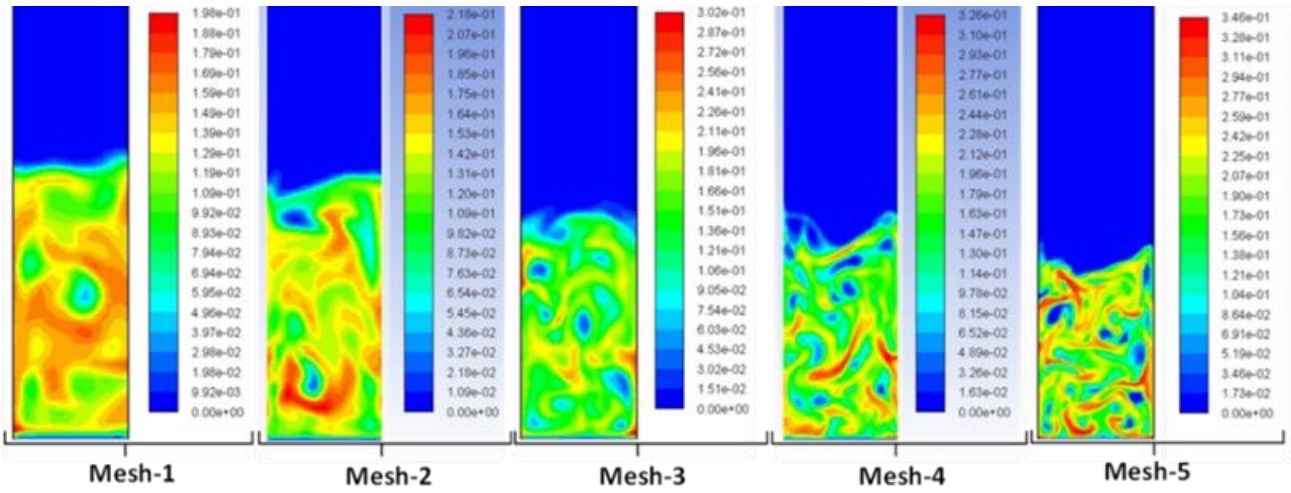

Fig. 3 Instantaneous volume fraction contours of particles for mesh study (20 s and 1.0 m/s velocity of superficial)

As governing equations, the mass and the momentum equations are resolved for each solid and gas phases (Ansys, 2011). In order to understand how turbulence fluctuations impact the fundamental conservation equations, a suitable turbulence model is required. The turbulence model used in this study is the commonly employed k-ε turbulence model (Launder & Spalding, 1972), providing useful insights into industrial flows with acceptable accurate. Solid phase fluctuations in fluid domain are explained by kinetic theory of granular flow (Gidaspow, 1994). It is necessary to calculate the solid phase pressures and viscosities based on granular temperature in order to determine the solid phase pressures and viscosities. It is crucial to comprehend that the temperature of the granular material is directly linked to the kinetic energy of the solid particles, which exhibit random motion. The Syamlal-O'Brien drag model is utilized for determining the interphase drag coefficient when calculating the overall drag coefficient. (Syamlal et al., 1993). Coefficients of specularity and restitution are determined to be 0.6 (Chang et al., 2013) and 0.95 (Chang et al., 2013; Alzate Hernández, 2016), respectively.

This study includes a series of CFD simulations to reveal hydrodynamic behaviors of the oxy-combustion process in the FCC regenerator by comparing them with air-combustion simulations. As part of the process of regenerating a coke-deposited catalyst, oxygen (24% O_2 + 76% CO_2) is transferred into the regenerator for the oxy-combustion process while air (21% O_2 + 79% N_2) is supplied into the regenerator for the air-combustion process. The same flow rate of gases was supplied to the regenerator at three different velocities (0.7 m/s, 1 m/s, 1.5 m/s) to compare oxy-combustion and air-combustion.

It can be seen in Fig. 2 that the surface of the regenerator that receives gas (210 mm in diameter) is determined to be a velocity inlet boundary condition, whereas the surface of the regenerator that leaves the gas (290 mm in diameter) is determined to be a pressure outlet boundary condition. For all surfaces, the wall boundary conditions are implemented as the no-slip condition for the gas phase and the partial slip condition for the solid phase. The time step size is 0.0005 s (Chang et al., 2016), and 20 iterations (Azarnivand et al., 2018) are conducted for each time step. The value of 0.001 is reached as a convergence criterion for all variables at the end of all simulations. The SIMPLE algorithm is employed as a method of coupling velocity and pressure for the numerical approach is used. First Order Upwind scheme was employed for variables such as turbulence kinetic energy (k) and turbulence dissipation ratio (ε) while for the time-dependent solution formulation is First Order Implicit. The solid phase that was analyzed in this research is composed of a mixture of particles whose average size is 0.00065 mm and their density was 1500 kg/m^3. During the simulations, solid-gas multiphase granular flow CFD models were developed, which were capable of allowing the volume fraction of the solid packing to be as high as 0.63 during the simulations. The regenerator inventory at the start of the project is 4.95 kg. A total of eight processors were utilized for each analysis in order to carry out parallel processing with 32 GB ram and 3.3 GHz processor.

3. RESULTS AND DISCUSSIONS

This study was undertaken to investigate the oxy-combustion process, integrating with the FCC regenerator, and compare it with air-combustion process, mostly with regard to its hydrodynamic behavior. There are basically two stages to the study: (i) the mesh study of the oxy-combustion process, which is crucial to all CFD simulations; (ii) the CFD simulations of both oxy-combustion and air-combustion based on the same flow rate condition of the process with different gas inlet velocity values.

3.1 Mesh Study

Mesh independence analyses on the mesh numbers were conducted based on the use of five distinct quantities that are listed in Table 1. The study that was conducted to investigate mesh independence primarily analyzed the results by examining contours of the volume fractions on the x-y plane of the FCC regenerator and the volume fractions at different heights of the bed. Figure 3 depicts the contours of particle volume fraction for five distinct

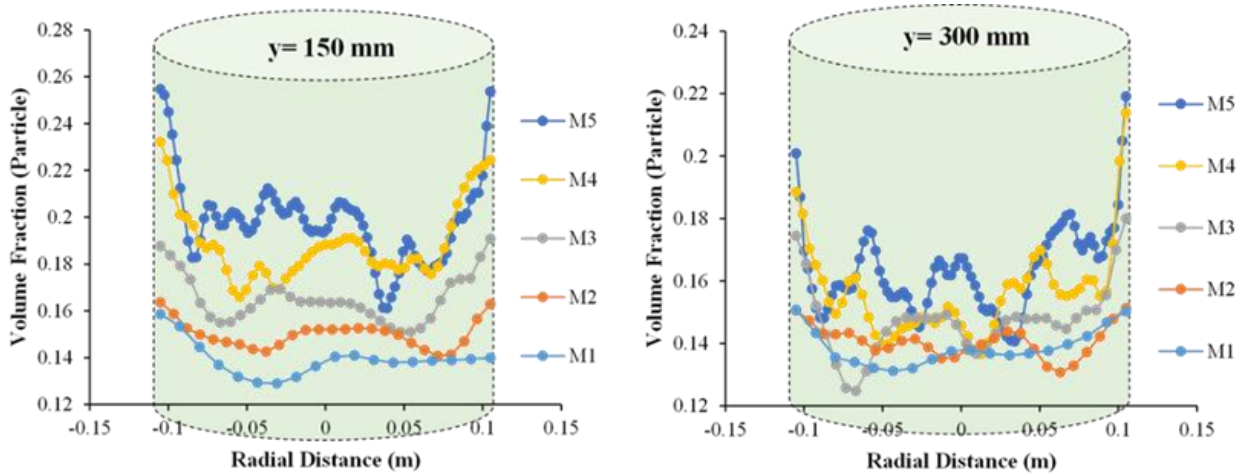

Fig. 4 The radial distribution of particles volume fraction with section-averaged for five meshes (under 1.0 m/s velocity of superficial, at 250 mm and 500 mm of bed density)

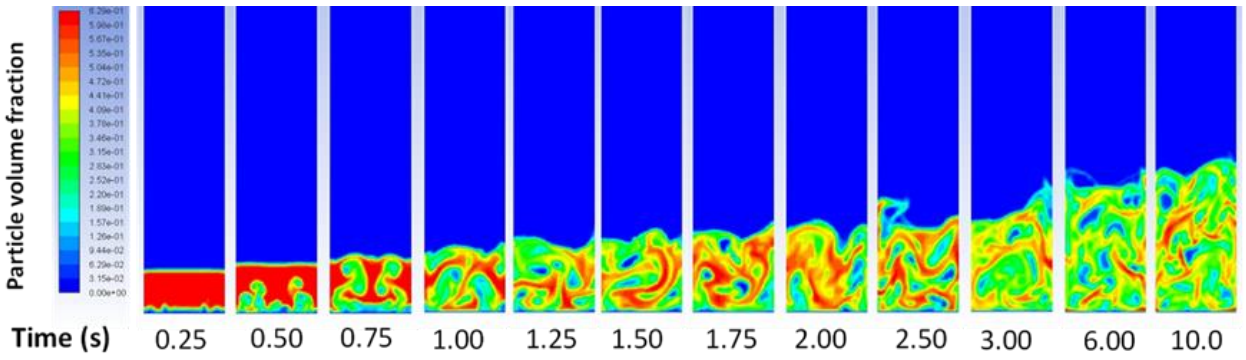

Fig. 5 The volume fraction contours of particles for M4 at an early stage of regenerator under 1.0 m/s gas inlet velocity

meshes with a gas inlet velocity of 1.0 m/s and an airflow duration of 20 s. Figure 4 displays the time-averaged (10-30 s) radial distribution of particle volume fraction with section-averaged at 150 mm and 300 mm for five different meshes with a gas inlet velocity of 1.0 m/s. With an increased mesh number, particles ascend with a lower height in the regenerator, as shown in Fig 3. Further, as the mesh structure becomes more sensitive, the magnitude of each variable at the center of each infinite volume, in the fluid domain, becomes more sensitive to the resolution. It should not be overlooked that this situation occurs when the flow time is 20 s as instantaneous, not a steady state condition. M4 and M5 particle distributions exhibit a close distribution, while M1, M2, and M3 meshes display a similar distribution across the regenerator but are distinct from distributions obtained for the other two mesh numbers, when both Fig. 3 and Fig. 4 are carefully examined. As a result of all these factors, M4 was credibly determined as a mesh number for this study's CFD models. Figure 5 shows particle volume fraction contours from an early stage of the regeneration process at 1.0 m/s gas inlet velocity under airflow.

3.2 Validation Study

A validation study was conducted to determine the applicability of the CFD model, used in this study, on the oxy-combustion process in the FCC regenerator. Reynolds number ($3.7*10^4$) was kept the same in validation simulation as in reference study. Using mesh studies as a basis, M4 mesh number was used in the validation study. In addition, it should be noted that solid-gas phase interactions within multiphase granular systems are revealed by the drag force (Li et al., 2009). Mesh number and turbulence model are therefore critical as well as the drag model in validation studies relating to multiphase granular flow structures. Comparing industrial data and previous study published by Chang et al. (2016), Fig. 6 shows the volume fraction throughout the dimensionless

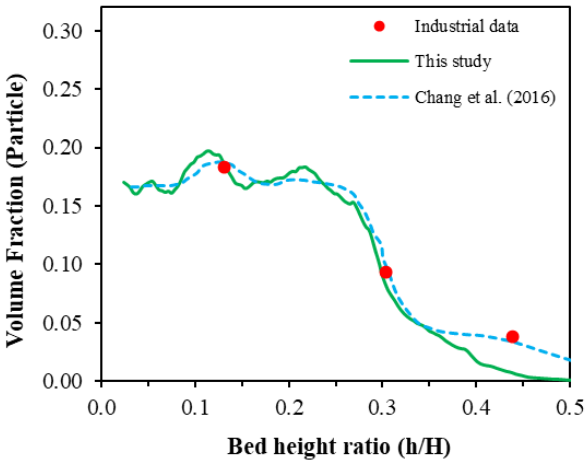

Fig. 6 Volume fraction values at different bed height ratios, comparing with industrial data and a reference study

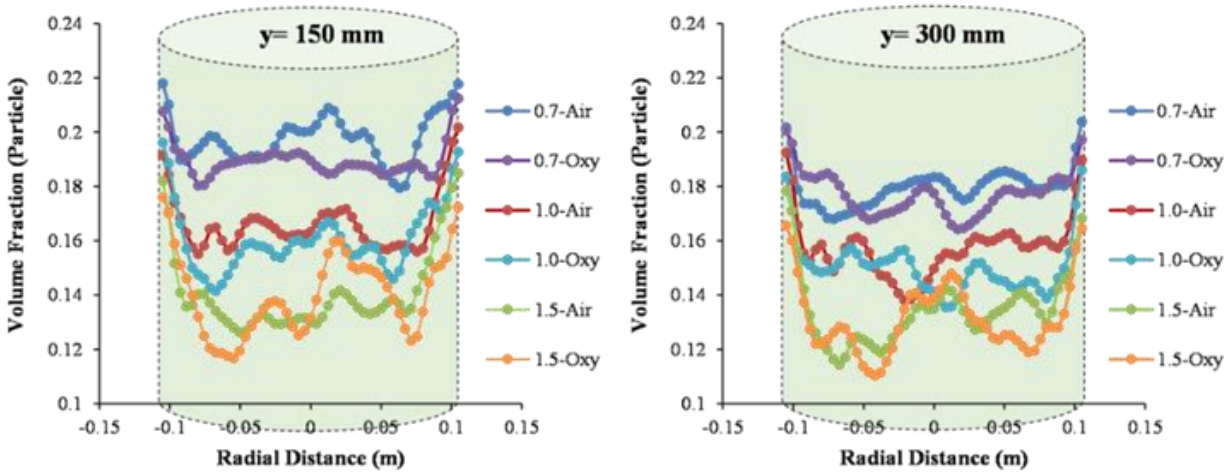

Fig. 7 The radial distribution of time-averaged particle volume fraction with section-averaged (0.7, 1.0, and 1.5 m/s velocity of superficial, at 250 mm and 500 mm of bed density)

bed height of the regenerator. Particularly, within the bottom section of the regenerator, the model employed in this investigation exhibits a strong agreement with the industrial data, consistent with the findings presented by Chang et al. (2016). Nevertheless, the computational fluid dynamics (CFD) model employed in this investigation exhibited an underestimation of particle volume fraction solely within the upper section (h/H > 0.35) of the regenerator when compared to the reference study. Based on the regenerator inventory capacity and pressure level, this is considered acceptable.

3.3 Same Inert Flow Rate Study

A primary difference between the air-combustion process and oxy-combustion is that the air-combustion process involves supplying $O_2 + N_2$ gas to the regenerator, while the oxy-combustion process involves transferring $O_2 + CO_2$ to the regenerator. The recycled CO_2 used in the oxy-combustion process would exhibit a similar volumetric flow rate to the N_2 present in the air when operated under identical conditions (De Mello et al., 2013). The regenerator would be able to extract more heat from carbon dioxide than from air because carbon dioxide has a higher heat capacity. CFD simulations were carried out in the FCC regenerator, examining three different gas inlet velocities to be able to understand the hydrodynamic nature of the process of oxy-combustion. All results of the oxy-combustion process obtained for this study from the CFD simulations are presented by comparing them with the results of the air-combustion process. Figure 7 illustrates the particle volume fractions averaged over a time period of 10-30s. These volume fractions are determined through radial distribution at two different heights of 150 mm and 300 mm, and at gas inlet velocities of 0.7 m/s, 1.0 m/s, and 1.5 m/s. The predictions are obtained for both air-combustion and oxy-combustion conditions. According to all simulation results in Fig. 7, zones near the center of the FCC regenerator have higher volume fractions than zones near the walls. FCC regenerator reactors feature this flow regime as one of their characteristics. There are several reasons why the volume fraction of the particles is higher between r = 0.9 m and the wall, including partial slip boundary conditions

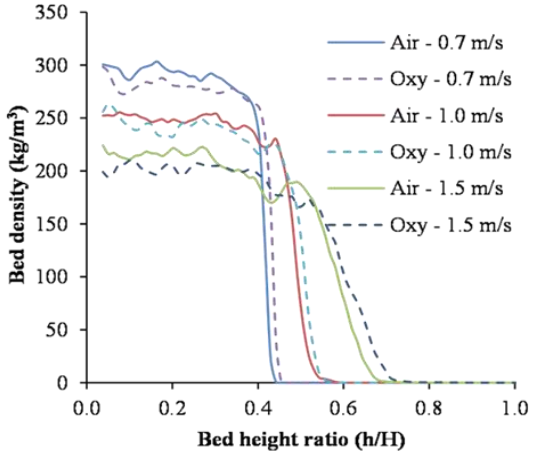

Fig. 8 The bed density profiles along the axial direction under air and oxy-combustion conditions at gas inlet velocities of 0.7, 1.0, and 1.5 m/s

and bubble formation, movement, and splitting (Gao et al., 2009). Figure 8 illustrates the averaged axial bed density profiles (10-30s) of the regenerator, comparing air and oxy-combustion scenarios at superficial velocities of 0.7, 1.0, and 1.5 m/s.

The observations in Fig. 8 reveal that the regenerator's bed density profiles can be divided into two distinct regions: (i) a dense phase with a bed density of 200-300 kg/m^3 at h/H ratio of 0.4, and (ii) a highly dilute phase with a bed density ranging from 0 to 200 kg/m^3 below the h/H ratio of 0.4. Moreover, as the gas inlet velocity increases, the drag force intensifies, leading to a reduction in bed density for both air-combustion and oxy-combustion processes. Meanwhile, CO_2 has a higher density than N_2, which occasions a higher drag force, this leads therefore to a low bed density value, especially, at the h/H=0-0.4 and a high bed density value above the h/H=0.4. Figure 9 presents the volume fraction distributions of the particles at 20 s for different gas inlet velocities (0.7, 1.0, and 1.5 m/s) during air and oxy-combustion processes. Considering the CFD simulations conducted with determined parameters, steady-state conditions could be reached for the solid-gas multiphase flow at the 20s. As shown in Fig. 9, when the color map bar is examined

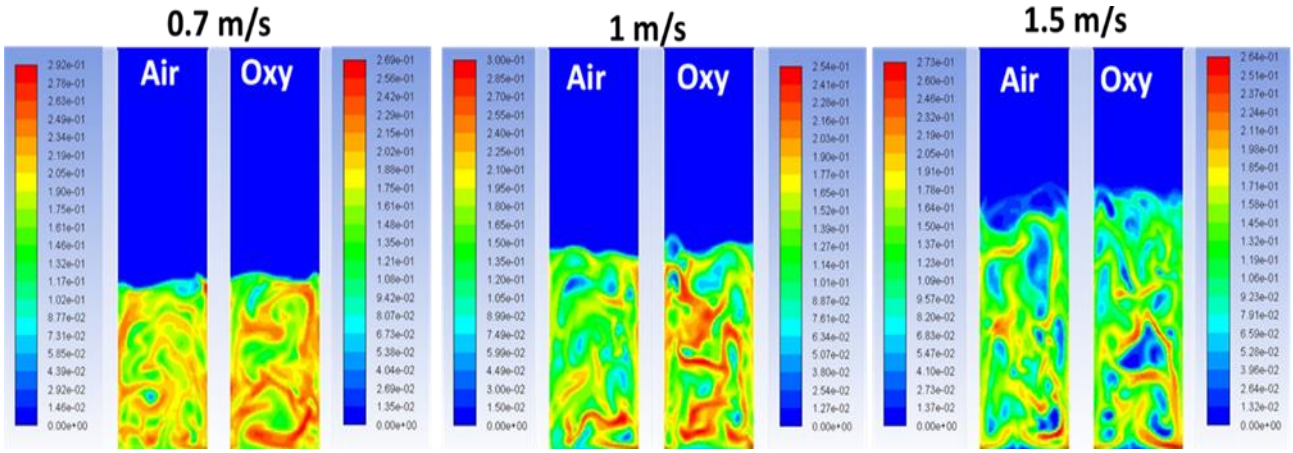

Fig. 9 The volume fraction contours of particles and velocity magnitude profiles (at 20s and 0.7, 1.0, and 1.5 m/s gas inlet velocities air-combustion and oxy-combustion)

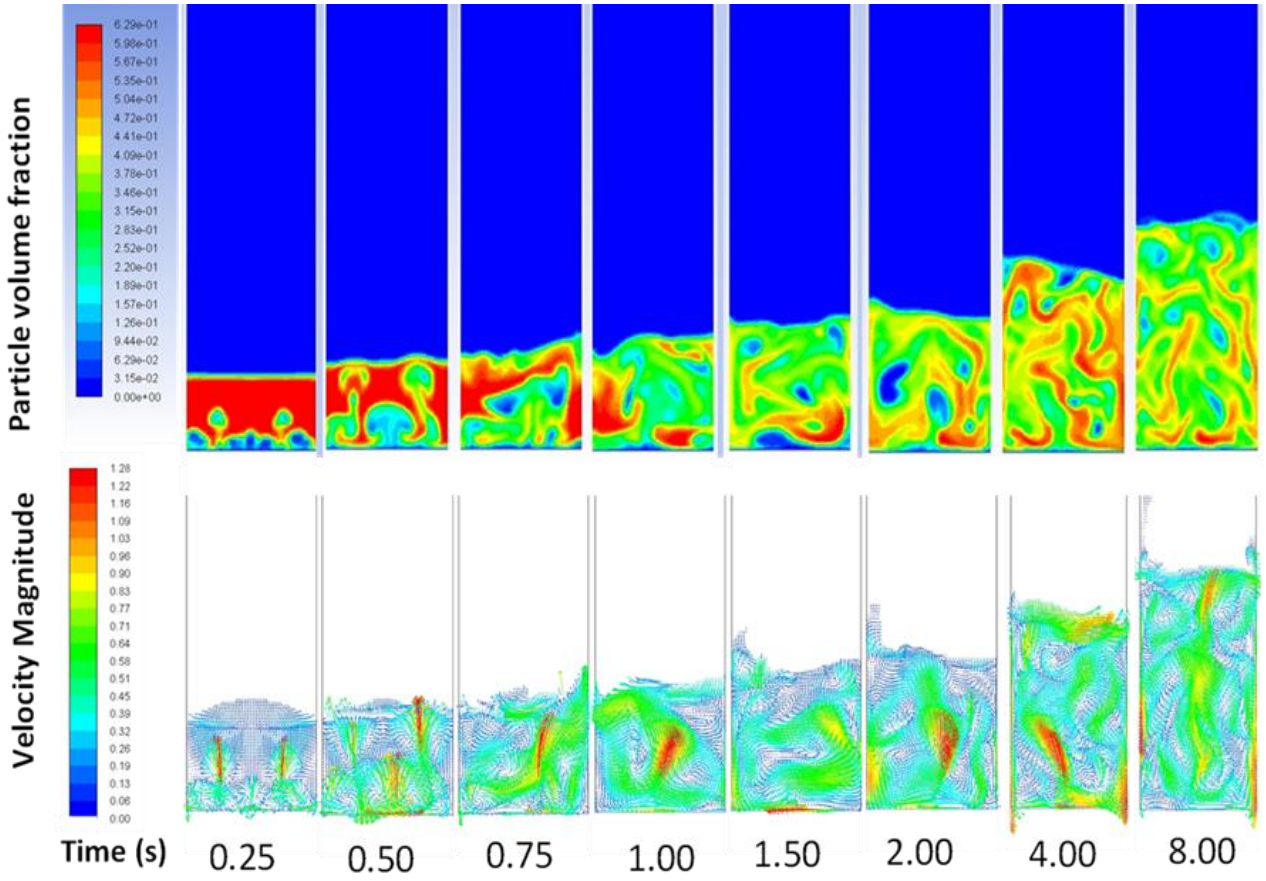

Fig. 10 The volume fraction contours of particles and velocity magnitude vectors at the early stage (1.0 m/s gas inlet velocity, air-combustion)

for each contour picture obtained for each gas inlet velocity, it can be seen that the maximum volume fractions differ. CO_2 drags the catalysts particles to more upper than N_2, which becomes more apparent as the gas inlet velocity increases. In addition, oxy-combustion bubbles exhibit horizontal expansion rather than vertical expansion like bubbles in air-combustion. Figure 10 illustrates the particle volume fraction contours and velocity magnitude vectors at the early-stage time intervals of reactor at the gas inlet velocity of 1.0 m/s under air-combustion. The particle volume fractions and velocity magnitude vectors at the steady state time intervals of reactor at 1.0 m/s of air-combustion are shown in Fig. 11. Considering that the velocity vectors of particles provide details about the particles, such as their movement direction, it is crucial to present them. Figure 12 depicts the particle volume fractions and velocity magnitude vectors at the early stage of reactor at the gas inlet velocity of 1.0 m/s under oxy-combustion. The particle volume fractions and velocity magnitude vectors at the steady state of reactor at 1.0 m/s of oxy-combustion are presented by Fig. 13. Usually, when simulating solid particle flow in multiphase granular flow regenerators, the duration of the steady-state period

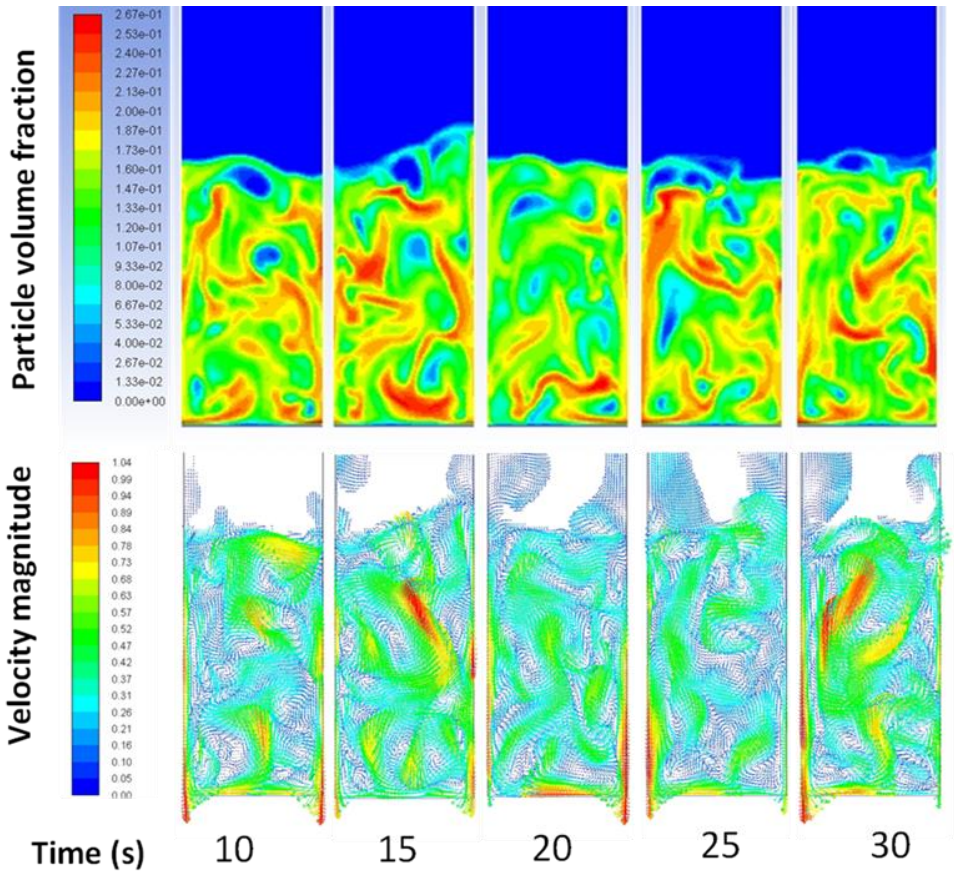

Fig. 11 The volume fraction contours of particles and velocity magnitude vectors at steady state (1.0 m/s gas inlet velocity, air-combustion)

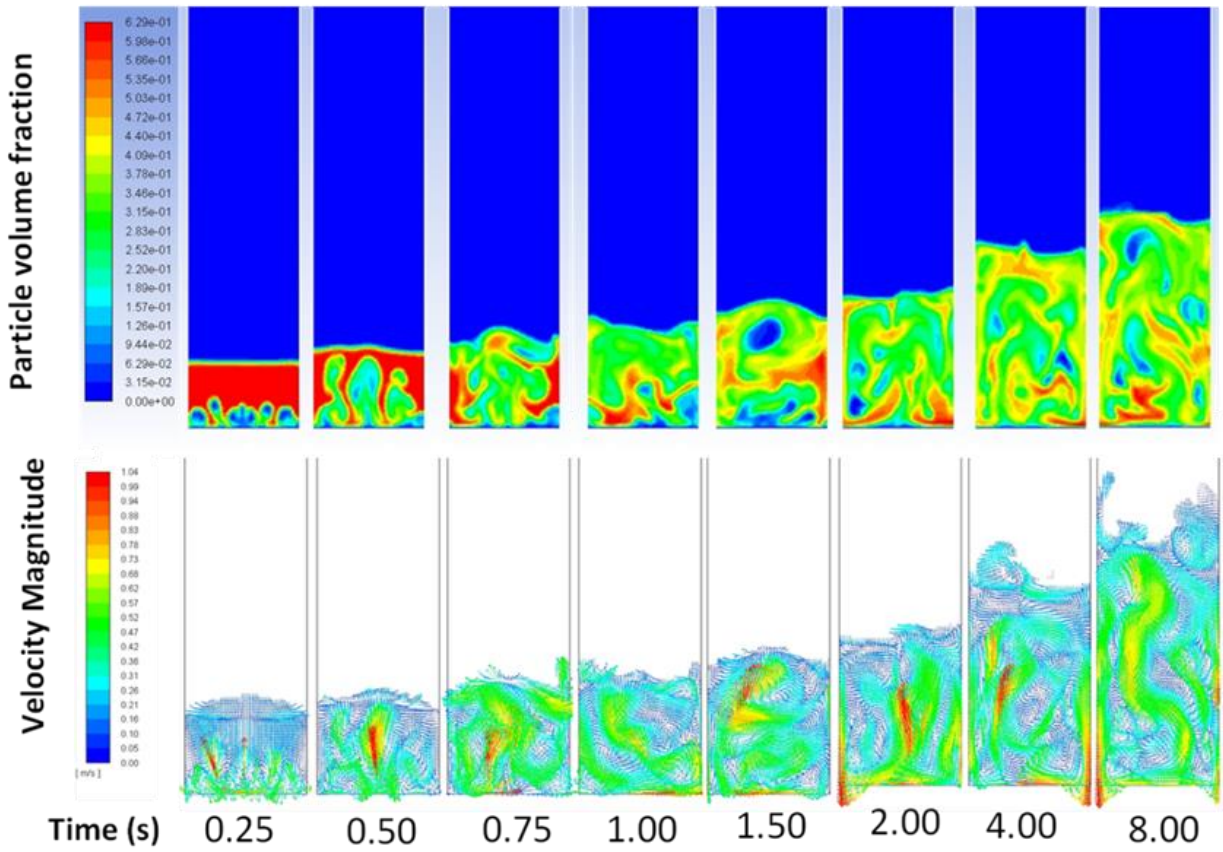

Fig. 12 The volume fraction contours of particles and velocity magnitude vectors at the early stage (1.0 m/s gas inlet velocity, oxy-combustion)

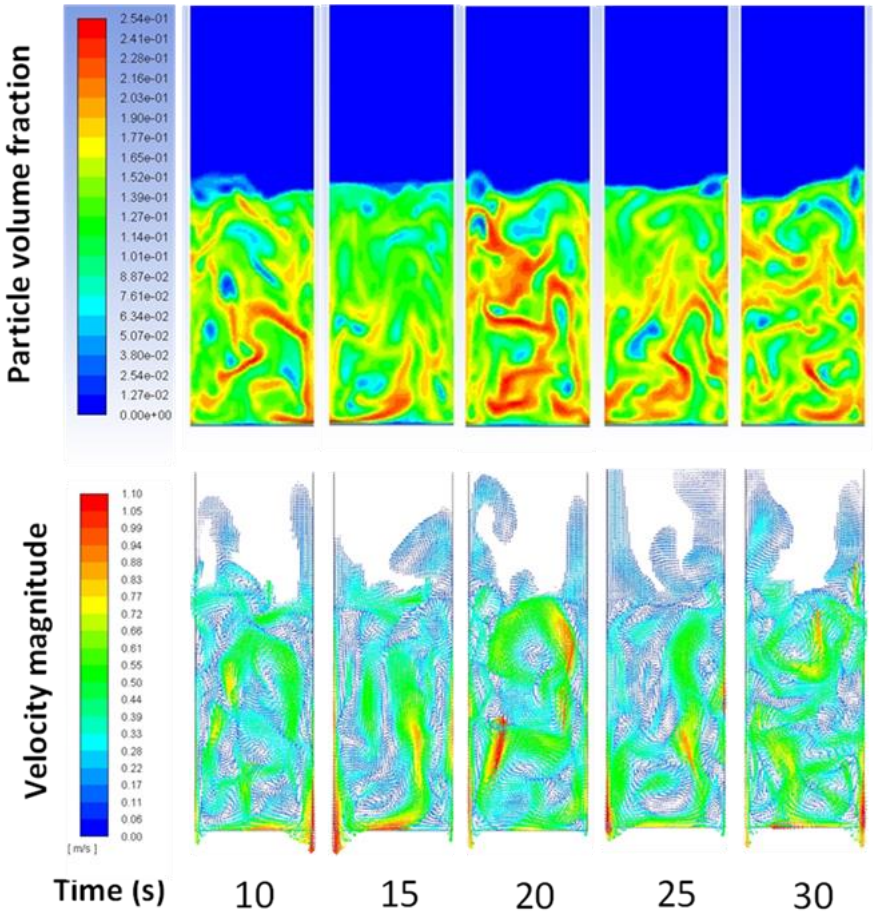

Fig. 13 The volume fraction contours of particles and velocity magnitude vectors at steady state (1.0 m/s gas inlet velocity, oxy-combustion)

is taken into consideration. In fact, the steady state time period of the flow simulation varies according to the geometry of the FCC regenerator and its size. Nevertheless, traditional FCC regenerators need to be temporarily deactivated and then reactivated in order to be maintained and cleaned. It is, therefore, necessary to gain a more in-depth understanding of the hydrodynamics involved at the early-stage of FCC regenerators, particularly in relation to solid-gas granular flow. As shown in Fig. 10 and Fig. 12, the volume contours for 0.25 s show that the bubbles separate from the flow volume at the inlet of the regenerator earlier in the air-combustion process compared to oxy-combustion. The turbulent flow exhibits an asymmetrical distribution even during the initial instants (0-0.5 s) following the commencement of both air-combustion and oxy-combustion processes. According to Fig 10-13, zones with bubbles within contour pictures correspond to areas with maximum velocity vectors within vector pictures. At this point, it is necessary to consider that the velocity vectors of all particles at these bubbles are not upwards and velocity vectors of some particles are downwards. In the early stage (0-8 s) of air-combustion process, Fig. 10 and Fig. 12 show that air-combustion process provides a relatively better bubble distribution than oxy-combustion process, while at steady-state flow time, Fig. 10 and Fig. 12 indicate that oxy-combustion process results in better mixing and distribution mechanisms. It can also be seen from Fig. 10 and Fig. 12 that at higher positions within the reactor, lower particle volume fractions are observed, suggesting the existence of dense and dilute phases in the lower and upper regions of the fluidized bed, respectively.

4. CONCLUSION

In this study, CFD simulations have been conducted on the solid-gas multiphase granular flow in the FCC regenerator when oxy-combusted coke-deposited catalysts are being regenerated in a solid-gas multiphase flow. A study was carried out to examine the impact of oxy-combustion process (O_2+CO_2 as gas mixing and FCC catalysts as solids) on the gas-solid hydrodynamics of FCC regenerators in comparison with those of air-combustion regenerators.

- Usually, in conventional drag calculations, the Syamlal-O'Brien model elucidates a transition from a dense phase to a subsequent dilution phase (ranging from 250 to 300 kg/m³). This phenomenon is particularly noteworthy when comparing the particle drag forces of CO_2 and N_2, wherein CO_2, owing to its higher specific gravity, exerts a notably greater drag force.
- Compared to industrial data and literature, the mesh number and turbulence model employed is demonstrated to be accurate, particularly up to a height of h/H > 0.35.
- In comparison to conventional air-combustion, oxy-combustion is characterized by a slight reduction in

the dense phase due to the expansion of the bed caused by the oxy-combustion gas. As a result of the introduction of gas to the regenerator that promotes the fluidization of solid particles, the mixing of solid particles is enhanced.

- When the gas inlet velocity is adjusted to 1.0 m/s, an optimal distributed flow pattern emerges across the dense phases, leading to the formation of vortices throughout these dense regions.

A thorough chemical and thermal CFD analysis would be valuable for further research in order to gain a deeper understanding of these systems. These analyses can focus on enhancing the residence time of the catalyst with coke deposits in the regenerator, particularly when operating under air and oxy-combustion conditions. The goal is to optimize this residence time for improved performance. Moreover, it is possible to forecast the influence of the carrier gas (CO_2) and the concentrations of flue gases (primarily CO_2 and H_2O, potentially including O_2 and CO) by studying the combustion of coke in oxy-combustion conditions.

CONFLICT OF INTEREST

The author declares no conflict of interest.

AUTHORS CONTRIBUTION

The author acknowledges complete accountability for the subsequent tasks: conceptualization and design of the study, conducting of simulations, analysis and interpretation of findings, and preparation of the manuscript.

REFERENCES

Aboudaoud, S., Touzani, S., Abderafi, S., & Cheddadi, A. (2023). CFD simulation of air-glass beads fluidized bed hydrodynamics. *Journal of Applied Fluid Mechanics*, *16*(9), 1778-1791. https://doi.org/10.47176/jafm.16.09.1742

Alzate Hernández, J. D. (2016). CFD simulation of an industrial FCC regenerator. *Escuela de Procesos y Energía*.

Amblard, B., Singh, R., Gbordzoe, E., & Raynal, L. (2017). CFD modeling of the coke combustion in an industrial FCC regenerator. *Chemical Engineering Science*, *170*, 731-742. https://doi.org/10.1016/j.ces.2016.12.055

Ansys, I. J. C. (2011). *Ansys Fluent theory guide*.

Azarnivand, A., Behjat, Y., & Safekordi, A. A. (2018). CFD simulation of gas–solid flow patterns in a downscaled combustor-style FCC regenerator. *Particuology*, *39*, 96-108. https://doi.org/10.1016/j.partic.2017.10.009

Berrouk, A. S., Huang, A., Bale, S., Thampi, P., & Nandakumar, K. (2017). Numerical simulation of a commercial FCC regenerator using multiphase particle-in-cell methodology (MP-PIC). *Advanced Powder Technology*, *28*(11), 2947-2960. https://doi.org/10.1016/j.apt.2017.09.002

Chang, J., Wang, G., Lan, X., Gao, J., & Zhang, K. (2013). Computational investigation of a turbulent fluidized-bed FCC regenerator. *Industrial & Engineering Chemistry Research*, *52*(11), 4000-4010. https://doi.org/10.1021/ie3013659

Chang, J., Zhao, J., Zhang, K., & Gao, J. (2016). Hydrodynamic modeling of an industrial turbulent fluidized bed reactor with FCC particles. *Powder Technology*, *304*, 134-142. https://doi.org/10.1016/j.powtec.2016.04.048

Chen, L., Ma, H., Ma, G., Pan, G., Li, P., & Sun, Z. (2022). Performance improvement prediction of push chain moist-mix concrete spraying machine employing orifice plate. *Journal of Mechanical Science and Technology*, *36*(6), 2889-2901. https://doi.org/10.1007/s12206-022-0521-z

Chu, K., & Yu, A. (2008). Numerical simulation of the gas− solid flow in three-dimensional pneumatic conveying bends. *Industrial & Engineering Chemistry Research*, *47*(18), 7058-7071. https://doi.org/10.1021/ie800108c

Cui, H., & Grace, J. R. (2007). Fluidization of biomass particles: A review of experimental multiphase flow aspects. *Chemical Engineering Science*, *62*(1-2), 45-55. https://doi.org/10.1016/j.ces.2006.08.006

Da Silva, T. C., Pinto, J. F., Santos, F. M., dos Santos, L. T., Aranda, D. A., Ribeiro, F., . . . Pereira, M. M. (2015). Vanadium and alumina modified with groups I and II elements for CO_2 and coke reaction under fluid catalytic cracking process. *Applied Catalysis B: Environmental*, *164*, 225-233. https://doi.org/10.1016/j.apcatb.2014.09.028

De Mello, L. F., Gobbo, R., Moure, G. T., & Miracca, I. (2013). Oxy-combustion technology development for Fluid Catalytic Crackers (FCC)–large pilot scale demonstration. *Energy procedia*, *37*, 7815-7824. https://doi.org/10.1016/j.egypro.2013.06.562

Digne, R., Feugnet, F., & Gomez, A. (2014). A technical and economical evaluation of CO_2 capture from fluidized catalytic cracking (FCC) flue gas. *Oil & Gas Science and Technology-Revue d'IFP Energies nouvelles*, *69*(6), 1081-1089. https://doi.org/10.2516/ogst/2013209

Dos Santos, L. T., Santos, F. M., Silva, R. S., Gomes, T. S., Esteves, P. M., Pimenta, R. D., . . . Pereira, M. M. (2008). Mechanistic insights of CO_2-coke reaction during the regeneration step of the fluid cracking catalyst. *Applied Catalysis A: General*, *336*(1-2), 40-47. https://doi.org/10.1016/j.apcata.2007.10.005

Erdoğan, A., & Daşkın, M. (2023). Comparing of CFD contours using image analysing method: a study on velocity distributions. *Black Sea Journal of Engineering and Science*, *6*(4), 633-638. https://doi.org/10.34248/bsengineering.1310711

Fluent, A. (2009). *ANSYS Fluent 12.0 user's guide*. Ansys Inc, 15317, 1-2498.

Gao, J., Lan, X., Fan, Y., Chang, J., Wang, G., Lu, C., & Xu, C. (2009). Hydrodynamics of gas–solid fluidized bed of disparately sized binary particles. *Chemical Engineering Science*, *64*(20), 4302-4316. https://doi.org/10.1016/j.ces.2009.07.003

Gidaspow, D. (1994). *Multiphase flow and fluidization: continuum and kinetic theory descriptions*. Academic press. https://doi.org/10.1016/0032-5910(95)90055-1

Güleç, F., Meredith, W., Sun, C. G., & Snape, C. E. (2019). A novel approach to CO_2 capture in fluid catalytic cracking-chemical looping combustion. *Fuel*, *244*, 140-150. https://doi.org/10.1016/j.fuel.2019.01.168

Güleç, F., Meredith, W., & Snape, C. E. (2020a). Progress in the CO_2 capture technologies for fluid catalytic cracking (FCC) units—a review. *Frontiers in Energy Research*, *8*, 62. https://doi.org/10.3389/fenrg.2020.00062

Güleç, F., Meredith, W., Sun, C. G., & Snape, C. E. (2020b). Demonstrating the applicability of chemical looping combustion for the regeneration of fluid catalytic cracking catalysts. *Chemical Engineering Journal*, *389*, 124492. https://doi.org/10.1016/j.cej.2020.124492

Güleç, F., Erdogan, A., Clough, P. T., & Lester, E. (2021). Investigation of the hydrodynamics in the regenerator of fluid catalytic cracking unit integrated by chemical looping combustion. *Fuel Processing Technology*, *223*, 106998. https://doi.org/10.1016/j.fuproc.2021.106998

Güleç, F., & Okolie, J. A. (2023). Decarbonising bioenergy through biomass utilisation in chemical looping combustion and gasification: a review. *Environmental Chemistry Letters*, 1-27. https://doi.org/10.1007/s10311-023-01656-5

Güleç, F., Meredith, W., & Snape, C. E. (2023a). CO_2 capture from fluid catalytic crackers via chemical looping combustion: Regeneration of coked catalysts with oxygen carriers. *Journal of the Energy Institute*, 101187. https://doi.org/10.1016/j.joei.2023.101187

Güleç, F., Okolie, J. A., Clough, P. T., Erdogan, A., Meredith, W., & Snape, C. E. (2023b). Low-temperature chemical looping oxidation of hydrogen for space heating. *Journal of the Energy Institute*, 110, 101355. https://doi.org/10.1016/j.joei.2023.101355

Güleç, F., Okolie, J. A., & Erdogan, A. (2023c). Techno-economic feasibility of fluid catalytic cracking unit integrated chemical looping combustion–A novel approach for CO_2 capture. *Energy*, 284, 128663. https://doi.org/10.1016/j.energy.2023.128663

Hashim, M. Y., Abdelmotalib, H. M., Kim, J. S., Ko, D. G., & Im, I. T. (2020). A numerical study on gas-to-particle and particle-to-particle heat transfer in a conical fluidized bed reactor. *Journal of Mechanical Science and Technology*, *34*, 2391-2402. https://doi.org/10.1007/s12206-020-0516-6

Jones, D. S., & Pujadó, P. P. (2006). *Handbook of petroleum processing*. Springer Science & Business Media.

Kamer, M., Erdoğan, A., Tacgun, E., Sonmez, K., Kaya, A., Aksoy, I., & Canbazoglu, S. (2018). A performance analysis on pressure loss and airflow diffusion in a chamber with perforated V-profile diffuser designed for air handling units (AHUs). *Journal of Applied Fluid Mechanics*, *11*(4), 1089-1100. https://doi.org/10.29252/jafm.11.04.27699

Karabulut, K. (2023a). Heat transfer increment study taking into consideration fin lengths for CuO-water nanofluid in cross flow-impinging jet flow channels. *Thermal Science*, *(00)*, 35-35. https://doi.org/10.2298/TSCI221203035K

Karabulut, K. (2023b). Investigation of heat transfer improvements of graphene oxide-water and diamond-water nanofluids in cross-flow-impinging jet flow channels having fin. *Isı Bilimi ve Tekniği Dergisi, 43*(1), 11-30. https://doi.org/10.47480/isibted.1290668

Khan, M., Hussain, M., Mansourpour, Z., Mostoufi, N., Ghasem, N., & Abdullah, E. (2014). CFD simulation of fluidized bed reactors for polyolefin production–A review. *Journal of Industrial and Engineering Chemistry*, *20*(6), 3919-3946. https://doi.org/10.1016/j.jiec.2014.01.044

Launder, B. E., & Spalding, D. B. J. (1972). Lectures in mathematical models of turbulence. https://lccn.loc.gov/72083798

Li, P., Lan, X., Xu, C., Wang, G., Lu, C., & Gao, J. (2009). Drag models for simulating gas–solid flow in the turbulent fluidization of FCC particles. *Particuology*, *7*(4), 269-277. https://doi.org/10.1016/j.partic.2009.03.010

Li, S., & Shen, Y. (2022). Numerical simulation of multiphase flow in a full coal-direct chemical looping combustion process. *Chemical Engineering Science*, *248*, 117233. https://doi.org/10.1016/j.ces.2021.117233

Lu, F., Wei, K., Wang, M., Li, M., & Bao, H. (2023). Oil film deposition characteristics and judgment of lubrication effect of splash lubricated gears. *Journal of Mechanical Science and Technology*, 1-11. https://doi.org/10.1007/s12206-023-0415-8

Mezhericher, M., Levy, A., & Borde, I. (2012). Probabilistic hard-sphere model of binary particle–particle interactions in multiphase flow of spray dryers. *International Journal of Multiphase Flow*, *43*, 22-38. https://doi.org/10.1016/j.ijmultiphaseflow.2012.02.009

Miracca, I., & Butler, D. (2015). CO_2 capture from a fluid catalytic cracking unit: technical/economical evaluation. *Carbon Dioxide Capture for Storage in*

Deep Geologic Formations, eds KF Gerdes.(Gerdes: CPL Press), 67-81.

Pourahmadi, S., & Talebi, S. (2020). Hydrodynamic simulation of two-phase flow in an industrial electrowinning cell with new scheme. *Journal of Applied Fluid Mechanics*, *14*(1), 243-257. https://doi.org/10.47176/jafm.14.01.31207

Rautiainen, A., Stewart, G., Poikolainen, V., & Sarkomaa, P. (1999). An experimental study of vertical pneumatic conveying. *Powder Technology*, *104*(2), 139-150. https://doi.org/10.1016/s0032-5910(99)00056-x

Schwarz, M. P., & Lee, J. (2007). Reactive CFD simulation of an FCC regenerator. *Asia‐Pacific Journal of Chemical Engineering*, *2*(5), 347-354. https://doi.org/10.1002/apj.64

Singh, R., & Gbordzoe, E. (2017). Modeling FCC spent catalyst regeneration with computational fluid dynamics. *Powder Technology*, *316*, 560-568. https://doi.org/10.1016/j.powtec.2016.10.058

Syamlal, M., Rogers, W., & O'Brien, T. (1993). MFIX documentation: Volume 1, theory guide. *National Technical Information Service, Springfield, VA*. https://doi.org/10.2172/656644

Taghipour, F., Ellis, N., & Wong, C. (2005). Experimental and computational study of gas–solid fluidized bed hydrodynamics. *Chemical Engineering Science*, *60*(24), 6857-6867. https://doi.org/10.1016/j.ces.2005.05.044

Tang, G., Silaen, A., Wu, B., Fu, D., Agnello-Dean, D., Wilson, J., . . . Zhou, C. Q. (2017a). Numerical study of a fluid catalytic cracking regenerator hydrodynamics. *Powder Technology*, *305*, 662-672. https://doi.org/10.1016/j.powtec.2016.09.082

Tang, G., Silaen, A. K., Wu, B., Fu, D., Agnello-Dean, D., Wilson, J., . . . Zhou, C. Q. (2017b). Numerical simulation and optimization of an industrial fluid catalytic cracking regenerator. *Applied Thermal Engineering*, *112*, 750-760. https://doi.org/10.1016/j.applthermaleng.2016.10.060

Yang, Z., Zhang, Y., Liu, T., & Oloruntoba, A. (2021a). MP-PIC simulation of the effects of spent catalyst distribution and horizontal baffle in an industrial FCC regenerator. Part II: Effects on regenerator performance. *Chemical Engineering Journal*, *421*, 129694. https://doi.org/10.1016/j.cej.2021.129694

Yang, Z., Zhang, Y., Oloruntoba, A., & Yue, J. (2021b). MP-PIC simulation of the effects of spent catalyst distribution and horizontal baffle in an industrial FCC regenerator. Part I: Effects on hydrodynamics. *Chemical Engineering Journal*, *412*, 128634. https://doi.org/10.1016/j.cej.2021.128634

Zhang, S., Liu, N., Pan, Y., Wang, W., Li, Y., & Zhu, Y. (2021). Three-dimensional modelling of two-phase flow and transport in a pilot centrifugal spray dryer. *Chemical Physics Letters*, *765*, 138309. https://doi.org/10.1016/j.cplett.2020.138309

Zimmermann, S., & Taghipour, F. (2005). CFD modeling of the hydrodynamics and reaction kinetics of FCC fluidized-bed reactors. *Industrial & engineering chemistry research*, *44*(26), 9818-9827. https://doi.org/10.1021/ie050490+